frontiers | Frontiers in Immunology

TYPE Original Research
PUBLISHED 17 December 2024
DOI 10.3389/fimmu.2024.1499492

OPEN ACCESS

EDITED BY
Mariella Della Chiesa,
University of Genoa, Italy

REVIEWED BY
Stephen K. Anderson,
National Cancer Institute at Frederick (NIH), United States
Sytse Jan Piersma,
Washington University in St. Louis, United States

*CORRESPONDENCE
Katharine C. Hsu
hsuk@mskcc.org
M. Kazim Panjwani
panjwanm@mskcc.org

†PRESENT ADDRESS
Rosa Sottile,
Humanitas Clinical and Research Center, Pieve Emanuele, Italy
Kattria van der Ploeg,
Department of Medicine - Infectious Diseases,Stanford University School of Medicine, Stanford, CA, United States

RECEIVED 20 September 2024
ACCEPTED 19 November 2024
PUBLISHED 17 December 2024

CITATION
Panjwani MK, Grassmann S, Sottile R, Le Luduec JB, Kontopoulos T, van der Ploeg K, Sun JC and Hsu KC (2024) Single-cell profiling aligns CD56^{bright} and cytomegalovirus-induced adaptive natural killer cells to a naïve-memory relationship. *Front. Immunol.* 15:1499492. doi: 10.3389/fimmu.2024.1499492

Single-cell profiling aligns CD56^{bright} and cytomegalovirus-induced adaptive natural killer cells to a naïve-memory relationship

M. Kazim Panjwani[1*], Simon Grassmann[2], Rosa Sottile[1†], Jean-Benoît Le Luduec[1], Theodota Kontopoulos[1], Kattria van der Ploeg[1†], Joseph C. Sun[2] and Katharine C. Hsu[1,3*]

[1]Human Oncology and Pathogenesis Program, Sloan Kettering Institute, Memorial Sloan Kettering Cancer Center, New York, NY, United States, [2]Immunology Program, Sloan Kettering Institute, Memorial Sloan Kettering Cancer Center, New York, NY, United States, [3]Department of Medicine, Weill Cornell Medical College, New York, NY, United States

Development of antigen-specific memory upon pathogen exposure is a hallmark of the adaptive immune system. While natural killer (NK) cells are considered part of the innate immune system, humans exposed to the chronic viral pathogen cytomegalovirus (CMV) often possess a distinct NK cell population lacking in individuals who have not been exposed, termed "adaptive" NK cells. To identify the "naïve" population from which this "memory" population derives, we performed phenotypic, transcriptional, and functional profiling of NK cell subsets. We identified immature precursors to the Adaptive NK cells that are equally present in both CMV+ and CMV- individuals, resolved an Adaptive transcriptional state distinct from most mature NK cells and sharing a common gene program with the immature CD56^{bright} population, and demonstrated retention of proliferative capacity and acquisition of superior IFNγ production in the Adaptive population. Furthermore, we distinguish the CD56^{bright} and Adaptive NK populations by expression of the transcription factor CXXC5, positioning these memory NK cells at the inflection point between innate and adaptive lymphocytes.

KEYWORDS

natural killer cell (NK cells), HCMV (human cytomegalovirus), lymphocyte development and function, innate memory, single-cell RNA (scRNA) sequencing, human immunology

Introduction

The adaptive immune system has been classically defined by two features: expression of a unique antigen receptor, and the ability to form immunological memory (1). Conferring the ability of an immune cell to respond to a specific pathogen more quickly and robustly upon subsequent challenges following primary exposure, memory is linked to the antigen

receptor for teleological and technical reasons: endowing antigen specificity to the recall response and enabling the tracing of a single naïve clone's progeny following antigen exposure. However, the hallmark features of immunological memory - rapid and robust effector function, retention of proliferative capacity, and longevity - are grounded in the basic biology of a lymphocyte, and not just the expression of a rearranged protein sequence.

The contrast between the biology and the identification of immune memory is best demonstrated by the classification of immune cells: all adaptive immune cells are lymphocytes, but not all lymphocytes are adaptive immune cells, traditionally defined by surface expression of a rearranged antigen-specific receptor. Lymphocytes previously not encompassed by the adaptive immune system include natural killer (NK) cells, which do not express a unique, rearranged antigen receptor on their cell surface and are therefore traditionally considered innate lymphocytes. The presence of an NK cell subset with superior function following certain viral exposures, however, contradicts this classification. In mice infected with mouse cytomegalovirus (MCMV), a population of NK cells can proliferate rapidly, clear virally infected cells, contract, and then perform these same functions again when exposed to MCMV a second time (2). In a subset of humans with prior exposure to human CMV, there is an outgrowth of a stable NK subpopulation with homogenous patterns of activating and inhibitory receptor expression that responds robustly to CMV-infected fibroblasts *in vitro* (3–5). The distinction of NK cells from the adaptive immune cells on the basis of absence or presence of an antigen receptor is blurred by the expression of viral antigen-recognizing receptors found on some NK populations: in mice, Ly49H, which binds MCMV-derived m157 protein (6, 7); and in humans, NKG2C, which binds certain HCMV UL40-derived peptides presented on HLA-E (8, 9). In concession to their apparent capacity for expansion upon re-challenge with their respective cognate antigen (9, 10), these receptor-expressing subsets are often referred to as "memory-like" or "adaptive" NK cells.

The identification of an Adaptive NK precursor, an analog to the naïve T lymphocyte, has been limited by the absence of a universally accepted phenotypic definition for the Adaptive NK population itself in humans. Various combinations of the expression of NKG2C, CD57, self–MHC-specific KIR, high levels of CD2, DNAM-1, or CD16, and the absence of FcRγ, NKp30, NKp46, PLZF, or EAT2 have all been used to define this population (3, 5, 11–14). None of these features, however, is both exclusive to and necessary for Adaptive NK cells: NKG2C+ NK cells are present in CMV-seronegative (CMV-) individuals, and Adaptive NK cells have been found even in CMV+ individuals lacking the *KLRC2* gene encoding NKG2C (12). Thus, attempts at identifying Adaptive NK cells through single-cell RNAseq have been stymied by the reliance upon *KLRC2* expression to identify the cells. Heterogeneity confounds the evaluation of the functional capacity of Adaptive and other NK cell subsets; NK cells can be stimulated through multiple receptors that can be preferentially expressed by different subsets, thus biasing the response to any single stimulus (15). Furthermore, tracking of NK cells in response to infection *in vivo* is not routine in humans, hindering the identification of a precursor prior to exposure and tracing its differentiation into Adaptive and potentially other NK cell subsets.

Recently published work has relied upon single-cell sequencing of the human peripheral blood or tissues to generate atlases of human NK cells and other innate lymphocytes (16–18). These results provide a valuable resource for transcriptional classification, but are absent validation at the phenotypic and functional level in many cases and do not provide developmental insight. Robust definitions of NK cell populations are still needed to achieve concordance with current knowledge of lymphocyte biology and contribute to its further understanding.

Using a multimodal approach incorporating single-cell profiling at the transcript, protein, and functional level, we provide evidence that the relationship between a subset of the $CD56^{bright}$ and Adaptive NK cell populations fits the naïve-memory lymphocyte framework. We describe an immature precursor population present in CMV-naïve individuals, identify unique but tightly linked $CD56^{bright}$ and Adaptive NK transcriptional states that are distinct from the classic $CD56^{dim}$ NK population, and demonstrate the acquisition of priming-independent superior effector function and retention of proliferative capacity by the Adaptive NK population.

Results

Co-expression of NKG2A and NKG2C on immature NK cells independent of CMV exposure

Whereas NKG2C is neither necessary nor sufficient to define Adaptive NK cells, the receptor does recognize a CMV-derived peptide and the frequency of NK cells expressing it increases after CMV exposure in individuals who possess the gene. Therefore, we used NKG2C as a signifier for Adaptive potential or identity, rather than marking the strict boundary of the population. Among human peripheral blood NK cells, we found that a minority of NKG2C+ NK cells are both negative for CD57, a marker for presumed terminal differentiation (19–21), and positive for CD62L, a lymph organ homing molecule present on memory and naïve T cells and found on some NK cells (22–24) (Figure 1A). Further indicative of their immature status, the majority of these CD57-CD62L+ NKG2C+ NK cells co-expressed the inhibitory receptor NKG2A, whereas the majority of CD57+ or CD62L- NKG2C+ NK cells did not (Figure 1B). The presence of Adaptive NK cells is almost exclusive to individuals who are CMV seropositive (CMV+), a marker of CMV "antigen exposure"(3); however, these NKG2C+NKG2A+ (A+C+) NK cells were found in equal frequency among both CMV+ and CMV- individuals when surveying 142 healthy donors (Figure 1C). The copy number of the *KLRC2* gene encoding NKG2C is correlated with A+C+ frequency, indicating that their population frequency is intrinsic to the host genotype in addition to being independent of antigen exposure (Supplementary Figure S1A). The frequency of A+C+ NK cells is positively correlated with the frequency of A-C+ NK cells among CMV- individuals, but this association is lost in CMV+ individuals in whom the A-C+ population has undergone

10.3389/fimmu.2024.1499492

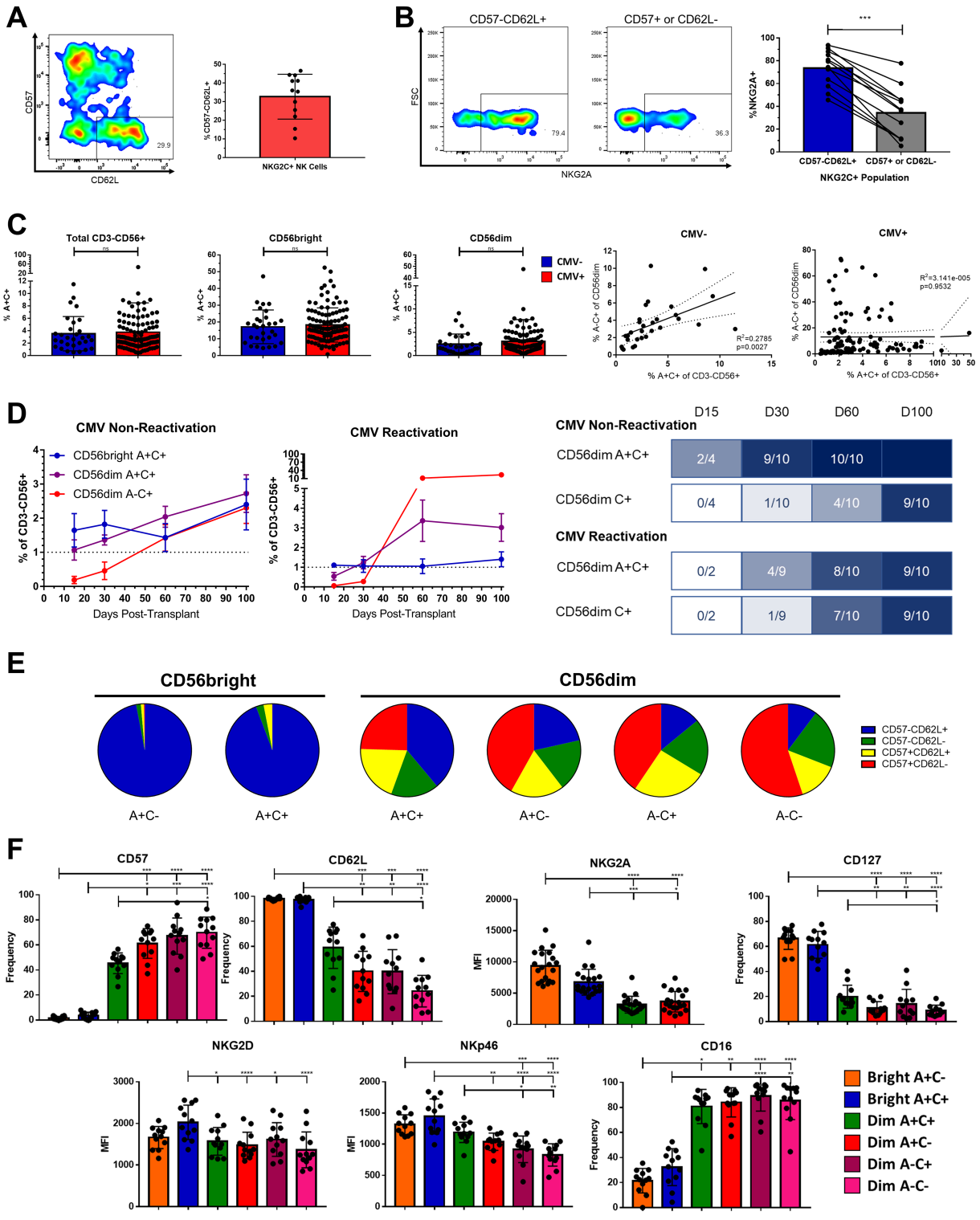

FIGURE 1
Phenotypic identification and characterization of an immature NKG2C+ precursor for Adaptive NK cells. **(A)** Left, expression of CD57 and CD62L on live CD3-CD56+NKG2C+ NK cells in a representative healthy donor. Right, frequency of CD57-CD62L+ cells among NKG2C+ NK cells; bar represents mean and SD. **(B)** Left, expression of NKG2A in NKG2C+ NK cell populations from a representative healthy donor. Right, frequency of NKG2A expression in NKG2C+ NK cell populations; lines connect paired donors, Wilcoxon matched pairs signed-rank test performed. **(C)** Left, frequency of A+C+ among indicated populations from either CMV-seronegative or seropositive healthy donors; Mann-Whitney Test performed. Right, frequency of A+C+ and A-C+ among $CD56^{dim}$ NK cells from CMV-seronegative or seropositive healthy donors; Spearman correlation coefficient shown. **(D)** Left, mean frequency of populations among total NK cells in peripheral blood of HSCT recipients with and without CMV re-activation in this timespan; N=10 each. Right, timelines showing fraction of the same recipients reaching reconstitution threshold of 1%. **(E)** Proportions of CD57 and CD62L expression among NK cell subsets from 12 healthy donors; mean represented. **(F)** Expression of cell surface markers on NK cell populations from healthy donors Dunn's multiple comparison test performed, comparing groups below tick marks to group below capped end. ns, not significant; * p <0.05, ** p <0.01, *** p <0.001, **** p<0.0001.

significant expansion (Figure 1C). Likewise, the amount of NKG2C on the cell surface NK cells is slightly higher in the CD56bright A+C+ population than in the CD56dim A+C+ and A-C+ populations in CMV- individuals, but the level is dramatically increased in the CD56dim A-C+ population of CMV+ individuals (Supplementary Figure S1B), likely as a consequence of clonal expansion of NKG2C^{hi} clones. Using human post-hematopoietic stem cell transplant immune reconstitution as a model of *in vivo* development, we found that A+C+ NK cell reconstitution precedes or is concurrent to A-C+ NK cell reconstitution in transplant recipients, supporting A+C+ NK cells as a likely developmental prerequisite for the A-C+ NK cell population (25) (Figure 1D).

Although transient upregulation of NKG2A on mature NKG2C+ NK cells in the presence of IL-12 has been reported (26), the phenotype of these A+C+ cells at baseline from healthy donors indicates they are not solely mature. A+C+ NK cells make up only 3.7% of the total CD3-CD56+ population but compose a substantial frequency of the CD56^{bright} population (18.0% vs 2.9% of the CD56^{dim} in all individuals). Like the CD56^{bright} A+C- cells, the CD56^{bright} A+C+ NK cells are almost entirely CD57-CD62L+, supporting their immature status (Figure 1E). Even among the CD56^{dim} NK cells, the A+C+ population is composed of a higher proportion of CD57-CD62L+ cells than the other 3 subsets of CD56^{dim} NK cells (A+C-, A-C+, A-C-). The phenotype of the A+C+ populations fills in a gradient between the CD56^{bright} and CD56^{dim} NK cell populations in other markers in addition to CD57 and CD62L, including IL-7Rα (CD127), CD16, and the level of NKG2A surface expression (Figure 1F). Despite expressing both NKG2A and NKG2C on the cell surface, expression of their common heterodimeric partner CD94 is not higher in A+C+ NK cells than in NK cells expressing only NKG2A (Supplementary Figure S1C), likely as a consequence of the subtle lowering of NKG2A expression as NK cells mature (27, 28) and gain expression of NKG2C.

The expression of activating receptors on these A+C+ NK cells correlates with their function against tumor targets with the cognate ligands: increased degranulation and IFNγ production against the NK-sensitive K562 and 721.221 lines, and intermediate response to ADCC of BE(2)n cells labeled with anti-GD2 antibody (Supplementary Figure S1D). As the activating receptor NKG2C and inhibitory receptor NKG2A both recognize the HLA-E:peptide complex (29), we challenged NK cells with K562 cells expressing equal amounts of HLA-E loaded with different peptides (Supplementary Figure S1E). We found that inhibition from NKG2A was dominant, but the degree of inhibition appeared to be peptide-sensitive; among CD56^{dim} A+C+ and A+C- NK cells, in which the expression of NKG2A is similar, inhibition by HLA-E:G*01 was modestly mitigated in the NK cells co-expressing NKG2C, suggesting signaling contribution from the activating receptor partially offsets the inhibition via NKG2A.

Adaptive NK cells possess a distinct transcriptional profile

As the A+C+ NK population appears to be a CMV-independent precursor to the Adaptive NK cell population, we sought to elucidate the relationship between these populations and the other peripheral blood NK cell populations through single-cell RNAseq. NK cells from two CMV+ healthy donors were sorted according to expression of CD56, NKG2A, and NKG2C, labeled with corresponding hashtag oligos, and then recombined in equal numbers to overcome the relative rarity of some populations (Supplementary Figure S2A). The CD56^{dim} A-C+ NK cells were segregated phenotypically further into either a subset with two additional features of adaptiveness (NKp30-FcRγ-, "Adaptive") or a subset with the inverse phenotype (NKp30hiFcRγ+, "non-Adaptive") which is found also in CMV- individuals (3, 10). There is evidence that FcRγ expression is destabilized and becomes dynamic in Adaptive NK (30, 31), such that FcRγ- would indicate an Adaptive NK while FcRγ+ would not necessarily preclude it. Nonetheless, transcriptional clustering would be expected to resolve the true identities of the FcRγ+ NK cells. Data from the two donors were analyzed separately to avoid sex differences or weighting from a dominant donor, and consistent results between the donors were examined further.

The overall structure of the UMAP constructed from the transcriptomes is consistent between the two donors (Figure 2A; Supplementary Figure S2B). Using the hashtag oligos to trace back the phenotypic origin of the individual cells, there are three major groupings of the phenotypic populations: the CD56^{bright} A+C- and CD56^{bright} A+C+ group together; almost the entire A-C+ NKp30- "Adaptive" population is joined by half of the A-C+ NKp30hi "non-Adaptive" population to form the second group; and the other half of the A-C+ NKp30hi "non-Adaptive" A-C+ NK cells co-localizes with the remaining CD56^{dim} populations (A+C-, A+C+, and A-C-) for the third group. Recently published CITE-seq work (16) aligns with these broad groups, referring to them as NK2, NK3, and NK1, respectively.

Driven by their phenotypic composition and their activation state, five common transcriptional clusters emerge among the peripheral blood NK cells: Bright, Classic Dim, Adaptive, Transitional Activation, and Type I IFN-stimulated (Figure 2B; Supplementary Figure S2C). Two additional clusters are present in one donor but not the other: a small T-Like population marked by expression of *CD3D* and *CD3G*, which have been observed in some Adaptive NK cells (32); and a centrally located cluster with no obvious distinguishing feature other than higher gene content. Using genes consistently upregulated and downregulated among the top 100 DEGs of the two donors, signatures were defined for each of the transcriptional clusters (Supplementary Table S1). The Bright cluster, containing much of the CD56^{bright} A+C- and A+C+ populations, express *SELL*, *IL7R*, *GZMK*, the chemokines *XCL1* and *XCL2*, and the transcription factors *MAFF* and *TCF7* (Supplementary Figure S2D; Figure 2B). The Classic Dim cluster, containing much of the diverse array of CD56^{dim} "non-Adaptive" phenotypic populations, is distinguished by the expression of effector accessory molecules such as *CST7* and *CD247* and the chemokine *CCL4*. The Adaptive cluster, containing all the phenotypic "Adaptive" and half of the phenotypic "non-Adaptive" populations, distinguishes itself with expression of *GZMH*, *IL32*, *CD52*, the chemokine *CCL5*, and HLA Class II; the Adaptive

10.3389/fimmu.2024.1499492

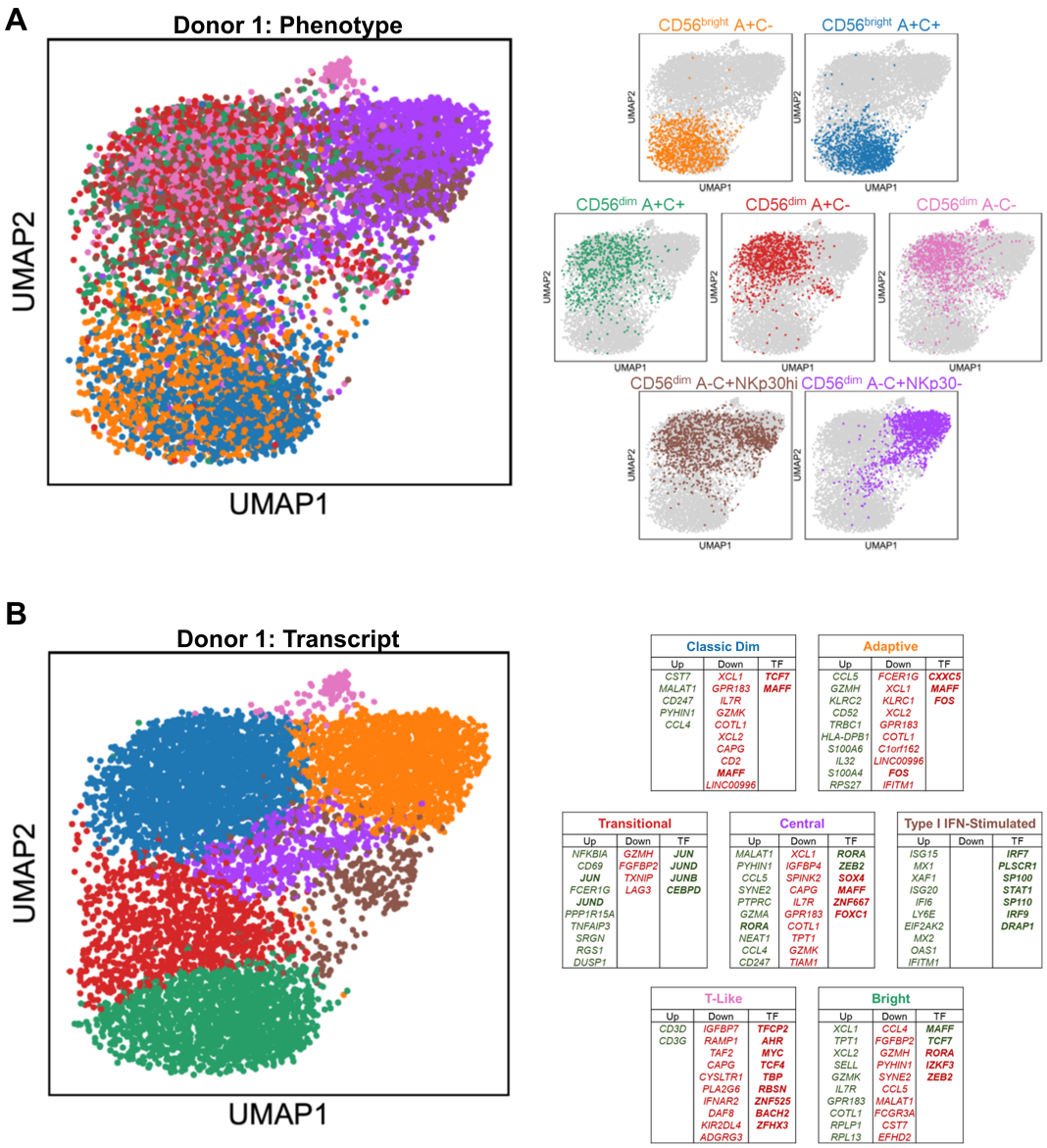

FIGURE 2
Distinct transcriptional profiles of CD56^{bright}, CD56^{dim}, and Adaptive NK cells. **(A)** Left, UMAP representation of peripheral blood NK cells from representative donor, color-coded according to phenotypic population hashtag. Right, individual phenotypic populations superimposed on total NK. **(B)** Left, UMAP representation of peripheral blood NK cells from representative donor, color-coded according to transcriptional cluster. Right, top 10 consistently upregulated (green), downregulated (red), and transcription factor (bold) genes among the top 100 DEGS of both donors for each transcriptional cluster; Central and T-Like clusters are unique to this donor.

transcriptional signature in the phenotypically "non-Adaptive" population indicates that residual or dynamic expression of proteins used to define these populations phenotypically can lead to misidentification without cross-validation. The Type I IFN-stimulated cluster is composed of all the phenotypic populations in roughly equal contribution, potentially revealing the dramatic effect this early pathogen detection signal has on the transcriptome to overwhelm all other differences. The Transitional Activation cluster, a mix of CD56^{bright} and CD56^{dim} cells also found in recent CITE-seq work (16), is distinguished by early response factors and negative feedback regulators such as *JUN*, *JUND*, *CEBPD*, and *NFKBIA*. Although these cells may be grouped together simply because of their activation status, localization to the Bright and Classic Dim interface and the dearth of Adaptive NK cells suggests a population-specific response and transitional state mediated by AP-1 factors and NFκB signaling. Velocity analysis implicates two possible transcriptional courses, both originating from the Bright cluster: one moves through the Transitional Activation stage onto Classic Dim followed by Adaptive, while the other passes through Type I IFN stimulation and onto Adaptive via a sparsely populated path (Supplementary Figure S2E); while similar transcriptional clusters were observed in the recent CITE-seq work (16), the exclusion of "NK3" (Adaptive NK) from trajectory analysis in that study likely explains the discrepancy in reported results.

10.3389/fimmu.2024.1499492

Adaptive and CD56^{bright} NK cells share a transcriptional program inverse of classic CD56^{dim} NK cells

A common feature of the UMAPs of both donors is the arrangement of these transcriptional clusters in the structure: the Bright (Green, Figure 2B; Supplementary Figure S2C), Adaptive (Orange), and Classic Dim NK cells (Blue) appear as vertices in this reduced representation, rather than lined up in a row. This formation, which has also been observed in recent single-cell datasets of human NK cells (16, 17), led us to the hypothesis that the transcriptional programs within these three clusters may have unique commonalities with each of the other two, rather than just a single vector of increasing maturation from Bright to Dim to Adaptive NK cells. The most intriguing of these possibilities was a link between the Bright and Adaptive NK cells, especially in the context of our earlier findings regarding the NKG2C+ CD56^{bright} NK cells. Our hashtagging strategy enabled us to further distinguish between the CD56bright NK cell populations and, as the Bright cells that were most outstretched toward the Adaptive were in fact the A+C+ population in our analysis, we considered the possibility that the signal from shared *KLRC2* expression was responsible for this observation. We removed *KLRC2* from the analysis to test this, but the overall structure remains preserved when controlling for this (Figure 3A). In contrast, removal of either the CD56^{bright} or CD56^{dim} A-C+ phenotypic populations collapses the structure (Supplementary Figure S3A, in contrast to Figure 2B; Supplementary Figure S2C). This underlying link between the Bright and Adaptive clusters is driven by the transcriptional program within NKG2C+ NK cells, not an artifact of *KLRC2* gene expression itself.

Although CD56^{bright} A+C- and CD56^{bright} A+C+ NK cells cluster together when analyzing the total peripheral blood NK cell population, a direct transcriptomic comparison of the two phenotypic populations confirmed that the CD56^{bright} A+C+ population is more akin to the Adaptive cells: increased expression of *GNLY*, *CD52*, and *IL32*, and decreased expression of *CLIC3*, *MAFF*, and *KLRB1* (Figures 3B, C, Supplementary Figures S3B, C; Supplementary Table S1). Similarly, a direct comparison of the Adaptive and Classic Dim transcriptional clusters uncovered additional DEGs shared by the Adaptive and Bright NK cells: increased expression of *CD2*, *CD3E*, *LINC01871*, *SELL*, and HLA Class II, and decreased expression of *HIPK2*, *TLE1*, *SH2D1B*, *ZBTB16*, *CHST2*, and *AKR1C3*. Several components of this common Bright-Adaptive gene set were validated at the protein level, including shared high levels of CD52, CD2 and HLA-II (Figure 3D). Another shared pattern are the ribosomal protein genes: among the over 80 genes, the overwhelming majority were expressed higher in Bright and Adaptive NK cells than in Classic Dim NK cells, despite equivalent gene and transcript count in these clusters (Supplementary Figure S3D). The canonical phenotypic differences between the Bright and Adaptive NK cells belie the common transcriptional program linking the two, including the preparation for intensive ribosomal biogenesis (33) – poised to generate an abundance of proteins for effector function, proliferation, or both.

A subset of NKG2C- NK cells exhibit shared adaptive-CD56^{bright} phenotypic features in CMV-seropositive individuals

Although CD56^{dim} A-C+ NK cells comprise the overwhelming majority of the Adaptive transcriptional cluster, NK cells from other phenotypic populations are also present in the Adaptive transcriptional cluster in small numbers (Figures 2; Supplementary Figures S2B, D). Exploring this further, we find that other CD56^{dim} NK cell populations (A+C-, A-C-, A+C+) also apparently lose FcRγ expression in a subset of cells following CMV infection (Supplementary Figure S4A), akin to the canonical CD56^{dim} A-C+ Adaptive population. Furthermore, the level of FcRγ protein expressed in the remaining FcRγ+ cells is lower following CMV infection, nearing the levels seen in CD56^{bright} NK cells, as also seen in the CD56^{dim} A-C+ Adaptive NK population. We therefore examined whether these FcRγ- NK cells following CMV exhibited other features of the shared Adaptive-CD56^{bright} phenotype, and found similar shifts in CD52, CD2, and CD161 expression (Supplementary Figure S4B). Together, these data indicate that NKG2C- NK cells, even when sufficient for the *KLRC2* gene, can also initiate an Adaptive program following CMV infection, and that the link between CD56^{bright} and Adaptive NK cells is preserved in these populations as well.

Adaptive NK cells are uniquely marked by loss of the transcription factor CXXC5, a marker of innateness

Memory is not simply the transient intermediate between immaturity and terminal differentiation, but a separate and stable state. The single-cell RNAseq data separate the Adaptive NK cell cluster from the other NK cells on a transcriptional basis. Although there are many similarities to the Bright cluster, unique to the Adaptive cluster is downregulation of the transcription factor *CXXC5* (Figure 4A). There are no reports of CXXC5 function in NK cells, but in other settings it has been shown to be a co-factor of TET2 and SUV39H1 (34–37) – epigenetic remodelers that repress memory and naïve-associated genes in T cells (34, 38, 39). Flow staining showed that CXXC5 protein is lower in the NKG2C+ NK cell population, but only in CMV+ individuals. Lower levels could also be seen in the subset of NKG2A- NK cells with an otherwise Adaptive phenotype (CD161-CD2hi, Figure 3D) in a CMV+ individual lacking the *KLRC2* gene (Figures 4B, C). Unlike PLZF, which is downregulated in both CD56^{bright} and Adaptive NK cells (Figure 4D), decreased CXXC5 is a unique marker of Adaptive NK cells. In fact, extending the analysis to T cells, we find that CXXC5 protein levels are highest in the NK-like NKG2C+ CD8+ T cell population, decreasing in the CD62L- effector populations, and lowest in the CD62L+ memory and naïve T cell populations, which essentially have none (Figure 4E). CXXC5 can therefore be a measure of innateness, with low expression of CXXC5 characteristic of the most adaptive of the NK cells.

10.3389/fimmu.2024.1499492

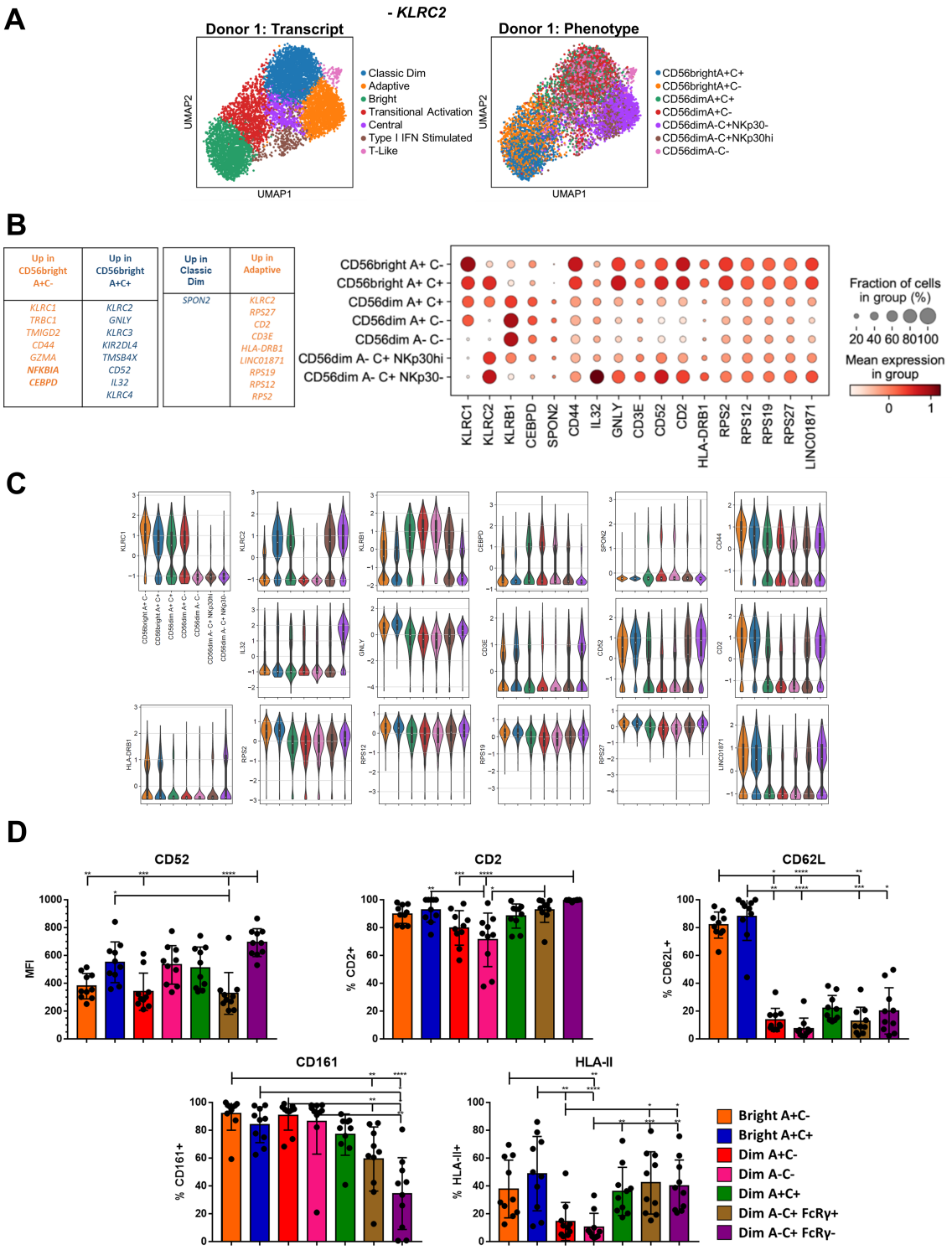

FIGURE 3
Convergence of a common Bright-Adaptive gene program. **(A)** UMAP of representative donor with *KLRC2* removed from analysis, color-coded according to transcriptional cluster (left) or phenotypic population (right). **(B)** Top DEGs between the CD56^{bright} A+C- and CD56^{bright} A+C+ phenotypic populations, and between the Classic Dim and Adaptive transcriptional clusters. Right, dot plot of selected DEGs in the indicated phenotypic populations in Donor 1. **(C)** Violin plots of selected gene expression in the indicated phenotypic populations in Donor 1; 25-75% IQR and median indicated by box and white dot, respectively. **(D)** Surface expression of proteins encoded by genes commonly expressed by Bright and Adaptive transcriptional clusters on NK cell populations from CMV+ donors. Dunn's multiple comparison test performed, comparing groups below tick marks to group below capped end. * p <0.05, ** p <0.01, *** p <0.001, **** p<0.0001.

10.3389/fimmu.2024.1499492

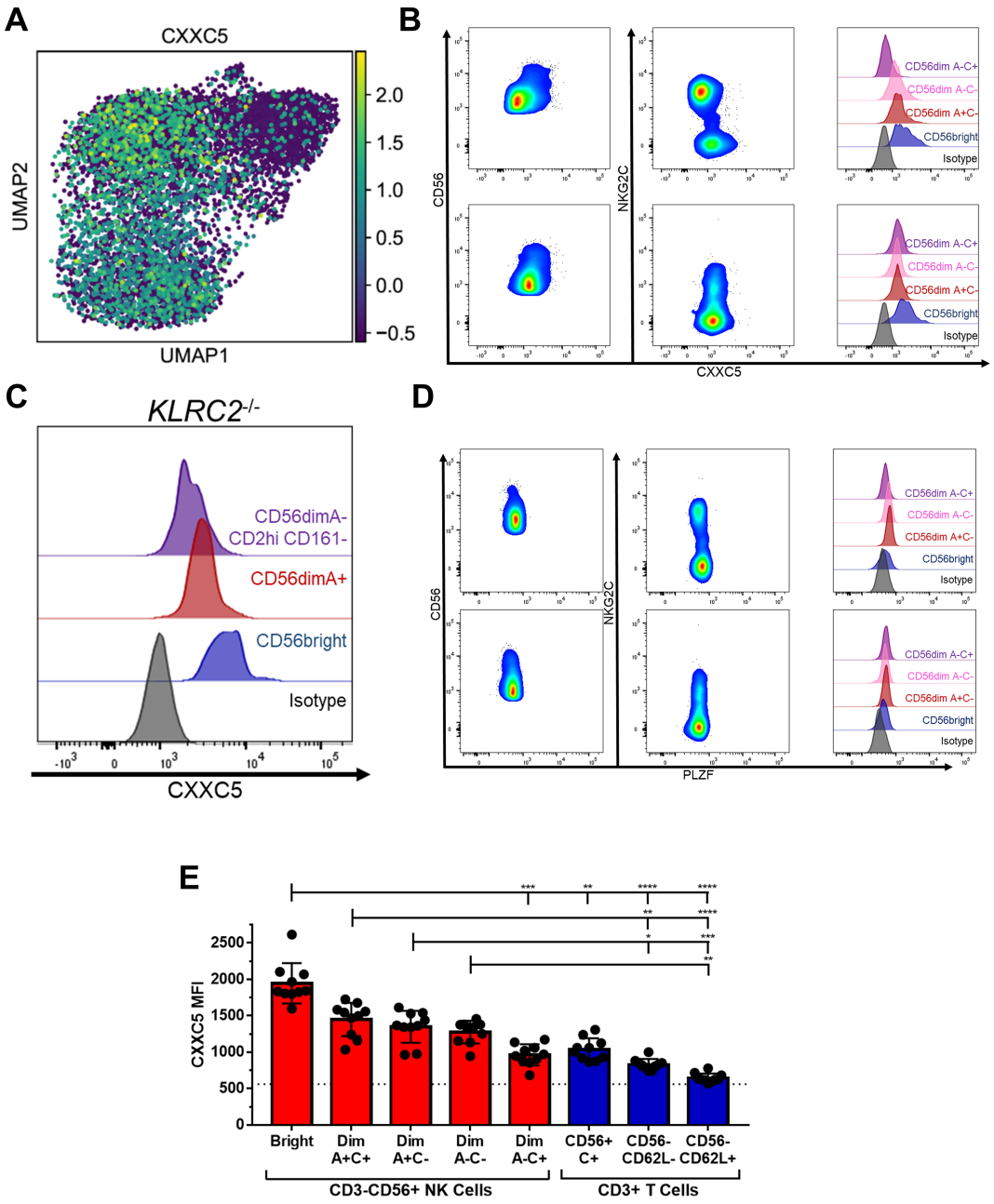

FIGURE 4
Bright and Adaptive NK Cells are distinguished from each other by expression of CXXC5. **(A)** Heatmap of *CXXC5* expression among Donor 1 NK cells. **(B)** Flow cytometry staining of NK cells for CXXC5 in representative CMV+ (upper) and CMV- (lower) donors. **(C)** Flow cytometry staining of NK cells for CXXC5 in a CMV+ donor with no copies of *KLRC2*. **(D)** Flow cytometry staining of NK cells for PLZF in representative CMV+ (upper) and CMV- (lower) donors. **(E)** Expression of CXXC5 in NK and T cell populations from CMV+ donors; dashed line represents isotype-matched control Ig staining. Dunn's multiple comparison test performed, comparing groups below tick marks to group below capped end. * p <0.05, ** p <0.01, *** p <0.001, **** p<0.0001.

Adaptive NK cells acquire superior effector function while retaining the capacity for proliferative burst

The metamorphosis from naïve to memory or effector cell is the tradeoff between a cell's self-renewal capacity and the speed and magnitude of its effector response. A fair comparison of NK cell responses to a target is challenging due to the diversity of receptors and ligands expressed heterogeneously across the various NK cell populations (15). To bypass the receptor-ligand biasing observed earlier with cellular targets (Figure 1F; Supplementary Figures S2B, C) and differences in cytokine receptor expression and thus sensitivity, we used an agnostic stimulus in the form of treatment with PMA and ionomycin and measured IFNγ production to assess total functional capacity (40–42); baseline *IFNG*, unlike the genes for granzymes and cytolytic molecules, was not among the top 100 DEGs for these

phenotypic populations or transcriptional clusters. After 5 hours of stimulation, a higher frequency of the CD56^{dim} A-C+ FcRγ- Adaptive population produced IFNγ than any of the other phenotypic populations (Figure 5A). NK cells expressing a self HLA-specific KIR produced more IFNγ than those not expressing a self HLA-specific KIR, indicating that the effect of education is not synapse-dependent (43, 44) (Figure 5B). The Adaptive NK cell population typically expresses CD57 and self HLA-specific KIR but is still superior to the other CD57+KIR+ CD56^{dim} NK cells (Figure 5C). The CD56^{bright} A+C-CD57-KIR- population produced less IFNγ than the equivalent CD56^{dim} A+C-CD57-KIR- population (Figure 5D). The low amount of IFNγ produced by the CD56^{bright} NK cells is surprising given how well they respond to tumor target lines in a co-culture functional assay (Supplementary Figure S1B). Unlike in the co-culture functional assay, the NK cells in this agnostic stimulus were not pre-treated with IL-2 so as to measure baseline capacity. Performing a time course of PMA and ionomycin challenge revealed that, when pre-treated with IL-2 overnight, the CD56^{bright} NK cells produce IFNγ as early as one hour after stimulus and respond consistently, while the CD56^{dim} NK cells accumulate their IFNγ response over time (Figure 5E). Whereas the CD56^{bright} cells require priming to respond, akin to the necessity of co-stimulation for naïve T cells (45, 46), the Adaptive NK cells have no such hindrance responding swiftly to a surrogate for activating receptor engagement.

The benefit of Adaptive NK cells and their functional superiority would be lost if they were unable to proliferate and form a long-lived niche. Addressing the same heterogeneity challenge, we stimulated peripheral blood NK cells with a lower dose of PMA and ionomycin. The Adaptive NK cells underwent robust and sustained proliferation after nine days of stimulation (Figure 5F); intriguingly, some of the FcRγ- cells that grew the most were CD57-, which are rare among Adaptive cells in circulation (Figure 5G). While Adaptive NK cells initiated cell division at a similar rate to A+C+ NK cells, the A+C+ NK cells underwent an average of one additional round of cell division. Therefore, the Adaptive NK cell population retains proliferative capacity while acquiring superior effector function.

Discussion

The close transcriptomic and phenotypic linkage between the Bright and Adaptive NK cell populations upends a linear model of human NK cell differentiation, introducing a second axis and branch of development. The CD56^{bright} A+C+ NK cells are central to this due to their increased expression of Adaptive features and Bright-Dim-blurring surface phenotype. The exact tipping point from this population to Adaptive NK cells – the why, where, and how this differentiation step occurs – is a subject critical for further study, both to understand memory formation across innate and adaptive lymphocytes and to faithfully generate this functionally superior subset of cells on-demand for therapeutic use.

The co-expression of NKG2A and NKG2C on this precursor population is particularly curious – both receptors signal in these cells, but it is unclear if ligation of either or both is central or even relevant to their further differentiation. The presence of Adaptive NK cells that are NKG2C- or that exist in individuals who lack the gene for NKG2C indicates that signaling through this receptor – and recognition of CMV antigens through it – while advantageous, is not absolutely necessary for their development. This dispensation of NKG2C would also imply that CMV, while potent, is not the sole driver of the Adaptive NK population. Nonetheless, the expression of CD62L among both the CD56^{bright} and Adaptive NK offers a tantalizing clue as to where to find this transition in persons undergoing a primary CMV infection: matched single-cell analysis of NK cells in lymphoid organs and peripheral blood would likely provide invaluable data to fill in the missing link. Indeed, a recent examination of innate lymphocytes in human tissues identified the presence of Adaptive NK in tonsils (18).

Overnight culture of NK cells with IL-12, IL-15, and IL-18 has been shown by many groups to markedly improve the function of NK cells (47, 48). These NK cells have a transcriptomic signature resembling CD56^{bright} NK cells (49), which may explain their association with memory/Adaptive NK cells despite the absence of many features of an Adaptive-specific phenotypic signature (50). Indeed, the many similarities between the Bright and Adaptive NK cells underscore a potential mechanistic role for their differences in delineating naiveness from memory. In one example, both populations express the long intergenic non-coding RNA *LINC01871*, in contrast to its absence in the classic CD56^{dim} population, while the Bright alone express *LINC00996*; the transcriptional program in common between the Bright and Adaptive could be mediated in part by the former, and the differences a consequence of the latter. Loss of the transcription factor CXXC5, a partner of the T cell memory repressors TET2 and SUV39H1 (34–37), in the Adaptive NK populations presents a parsimonious model for the gain of some memory features in this population. Even if CXXC5 does not play a central mechanistic role, its loss is a reliable indicator of the shift to an memory/adaptive program. This is especially the case considering that the Adaptive NK cell population expresses levels of CXXC5 similar to its TCR-expressing "twin," the NKG2C+ CD8+ TCRαβ+ population (51), placing them shoulder-to-shoulder at the border of innate and adaptive cytotoxic lymphocytes.

The dissociation between the surface phenotype and transcriptome of the NK cell populations is one of the most striking findings of this study. For example, the conglomeration of most CD56^{dim} NK populations as a single transcriptional cluster in our data and others (16, 17) is in defiance of their phenotypic diversity and even functional capacity. As an example, KIR+ NK cells are intrinsically superior producers of IFNγ than KIR- NK cells in our agnostic stimulus model, but that advantage may be regulated at the protein level, rather than dependent upon transcriptional shifts (43). Therefore, the few effector molecule DEGs may point to more fundamental differences in these populations' roles in the immune response, such as XCL1/2 from CD56^{bright} cells recruiting cross-presenting XCR1+ dendritic cells, or cystatin-F protecting Classic Dim NK cells from activation of their potent Granzyme B cargo. Especially curious was the co-localization of half the CD56^{dim} A-C+ NKp30hiFcRγ+ NK cells with the Classic Dim and half with the Adaptive NK cells; the latter

10.3389/fimmu.2024.1499492

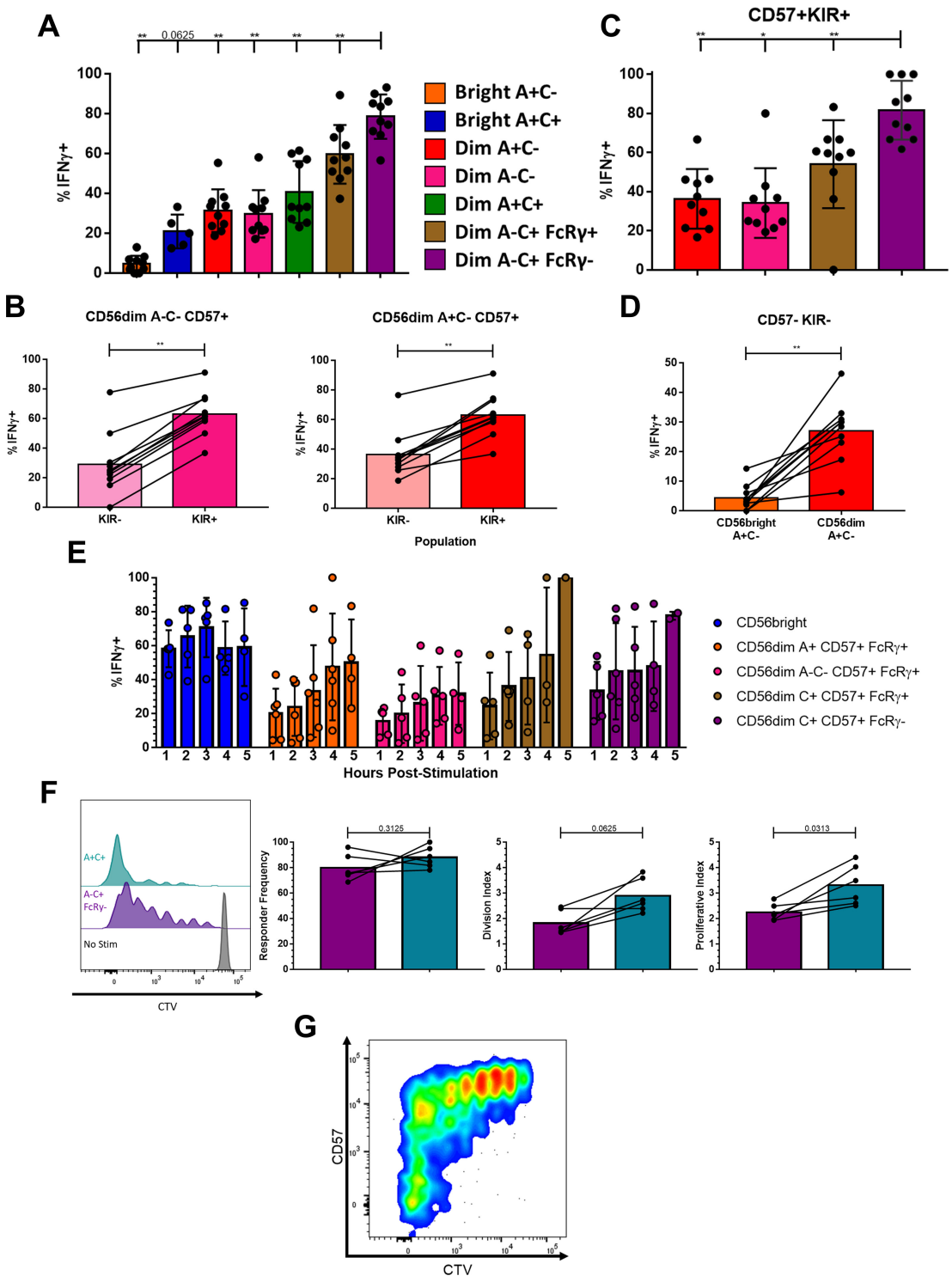

FIGURE 5
Memory-like effector function and proliferative capacity is intrinsic to Adaptive NK cells. **(A)** IFNγ production in NK cell populations from CMV+ donors following five hour stimulation with PMA+Ionomycin; Wilcoxon test performed on indicated pairs. **(B)** IFNγ production among NK cell populations expressing any one or more of KIR2DL1/2DS1/2DL2/2DS2/2DL3/3DL1/3DS1 or negative for all of these following five hour stimulation; Wilcoxon test performed. **(C)** IFNγ production in NK cell populations expressing CD57 and at least one self-recognizing KIR (KIR2DL2 and/or KIR2DL3) following five hour stimulation; Wilcoxon test performed on indicated pairs. **(D)** IFNγ production among NK cell populations negative for CD57 and KIR2DL1/2DS1/2DL2/2DS2/2DL3/3DL1/3DS1 following five hour stimulation; Wilcoxon test performed. **(E)** IFNγ production in NK cell populations at timepoints indicated following stimulation, after overnight culture with 200 U/mL IL-2. **(F)** NK cell populations nine days after stimulation. Left, dilution of proliferation dye in representative donor shown. Right, proliferation kinetics with lines connecting samples from the same donor; Wilcoxon test performed. **(G)** Expression of CD57 and proliferation dye among A-C+ FcRγ- NK cells nine days after stimulation with PMA+Ionomycin, representative donor shown. **(F, G)** Total CD3-CD56+ NK cell population shown as the distinction between $CD56^{bright}$ and $CD56^{dim}$ is lost after prolonged stimulation. ns not significant, * p <0.05, ** p <0.01.

had downregulated *FCER1G* expression below the technical limit of detection but still expressed FcRγ protein at that moment in time, a reminder that cell phenotype does not foretell fate.

Likewise, Adaptive NK cells express the phenotypic markers of maturity, such as CD56dim, CD57, and KIR, which would place them at the opposite end of the NK cell spectrum from Bright NK cells. However, the transcriptome tells a different story. The Bright and Classic Dim NK are radically different enough that some have speculated that they have different origins (16, 52), though the presence of a transitional population and shared somatic mutations (10) counters this. To progress from Bright to Classic Dim to Adaptive according to the traditional model of NK cell development, the NK cell would need to undergo a dramatic transcriptional and epigenetic reprogramming – and then undergo yet another dramatic reprogramming that largely reverses the first one. Early definitions of T cell memory were based on infection kinetics – antigen-experienced T cells that survived the effector contraction phase were deemed long-lived memory cells derived from the earlier effector population (53–55). However, increasing evidence has shown that the fate segregation of short-lived effector and long-lived memory progeny begins soon after antigen engagement (56–59), possibly as soon as the first cell division (60, 61). Our data nominate Bright NK as a similar bipotential progenitor for both Classic Dim and Adaptive NK. Moreover, we also note that our trajectory analysis and others' (17) indicate another, Classic Dim-Adaptive, pathway, suggesting at least two different origins – and perhaps types – of Adaptive NK cells (10).

A major implication of the Bright-Adaptive transition is the possibility of clonal expansion and maintenance among NK cells. In the absence of unique, heritable, and immutable rearranged antigen receptor sequences, clonal expansion has been inferred from strong data showing pools of Adaptive NK cells with shared patterns of chromatin accessibility and mitochondrial DNA somatic mutations within individuals, including mitochondrial somatic mutations shared between Adaptive NK and CD56^{bright} NK cells (10). On the other hand, the inflammatory environment of CMV infection has been shown to stunt the proliferation of Adaptive NK cells in response to IL-2 and IL-15 (30). One hypothesis to reconcile these results is that the signal supporting the outgrowth of this population synergizes with an activating receptor or comes after CMV is under control and the inflammation environment recedes, while another is the possibility of an unexplored "stem memory" population of Adaptive NK cells, such as the CD57- NKG2C+ FcRγ- population that expands in response to stimulus-agnostic PMA and ionomycin. Many immune cells besides B, T, and NK cells are permanently altered by pathogen exposure (62), but the "trained immunity" of macrophages, for example, is largely fungible between individual cells. An advantage of preserving an NK "clone" in the absence of a unique peptide-specific receptor is that the diversity of receptor expression across the NK cell compartment creates unique compositions of NK cell functional capacity (15), including individual cells that may be equipped to be highly effective in certain situations and further provided surrogate specificity through CD16-antibody interactions. Thus, a CD56^{bright} "naïve" NK cell expressing the CMV-recognizing receptor NKG2C may be shunted down a parallel track to form an effective, persistent, and self-renewing memory population to control a recurrent chronic viral infection.

Materials and methods

Flow cytometry

Extracellular staining for CD3 (BD, clone UCHT1: BrilliantViolet650), CD56 (Beckman Coulter, clone N901: ECD), CD8 (Biolegend, clone RPA-T8: BrilliantViolet570), NKG2A (Miltenyi, clone REA110: PE-Vio770), NKG2C (Miltenyi, REA205: APC, PE-Vio770, VioBright FITC; R&D, clone 134591: PE), KIR2DL1/S1 (Miltenyi, REA284: FITC), KIR2DL2/L3/S2 (BD, Clone CH-L: BrilliantViolet605, FITC), KIR3DL1/S1 (Miltenyi, REA168: APC-Vio770, FITC), CD57 (BD, clone HNK-1: BrilliantViolet421, PE), CD62L (Biolegend, clone DREG56: BrilliantViolet785; Beckman Coulter, clone DREG56: PE), NKG2D (Biolegend, clone 1D11: BrilliantViolet605), CD16 (BD, clone 3G8: BrilliantViolet711), NKp46 (Biolegend, Clone 9E2: PerCP-Cy5.5), NKp30 (Miltenyi, clone AF29-4D12: PE), CD2 (Biolegend, clone RPA-2.10: BrilliantViolet711), CD52 (Miltenyi, clone REA164: VioBlue), CD161 (Miltenyi, clone REA631: PE), HLA-DR/DP/DQ (Miltenyi, clone REA332: APC-Vio770), CD107a (BD, clone H4A3: BrilliantViolet786), CD14 (Biolegend, clone 63D3: AlexaFluor700; Miltenyi, clone TÜK4: FITC), CD4 (Biolegend, clone SK3: AlexaFluor700), TCRVδ1 (Miltenyi, clone REA173: APC-Vio770), PD-1 (Biolegend, clone EH12.2H7: PacificBlue), KIR3DL1 (BD, clone DX9: BrilliantViolet711), TCRγδ (eBioscience, clone B1.1: PE), KIR2DL1/S1 (Beckman Coulter, clone EB6B: PE-Cy5.5) was performed at room temperature for 30 minutes in PBS (without Ca or Mg) with 0.5% BSA and 2 mM EDTA. Intracellular staining for IFNγ (BD, clone B27; AlexaFluor700) and FcRγ (Millipore, rabbit polyclonal against FcERI γ subunit; FITC) was performed after fixation and permeabilization with Fix & Perm Cell Permeabilization Reagents (Life Technologies) according to manufacturer's instructions. Transcription factor staining for CXXC5 (Cell Signaling, clone D1O4P; labeled with anti-rabbit IgG (H+L) F(ab')^2 AlexaFluor647, Cell Signaling) and PLZF (eBioscience, clone Mags.21F7; AlexaFluor488) was performed using the FoxP3/Transcription Factor Staining Buffer Set (eBioscience) according to manufacturer's instructions. Viability was assessed by staining with DAPI (Sigma) or Live-Dead Fixable Aqua (Invitrogen). Analysis of flow data was performed in FlowJo 10.8.0 (BD).

Cell culture

PBMCs were isolated from buffy coats obtained from healthy volunteer donors via the New York Blood Center (NYBC). The MSKCC Institutional Review Board (IRB) waived the need for additional research consent for anonymous NYBC samples. Human donors *KLRC2* copy number was determined by PCR (63). PBMC were cryopreserved in fetal bovine serum with 10% DMSO. K562, 721.221, and BE(2)n (provided by Dr. Nai-Kong Cheung) cells were

tested regularly for mycoplasma via PCR. The HLA-E:G*01 construct was designed and expressed in K562s as described previously (51); the HLA-E:A*02 construct (leader sequence MAVMAPRTLVLLLSGALALTQTWA) from Genscript was designed and expressed in a similar fashion (51). All cells were cultured in RPMI 1640 with 10% FCS and Penicillin-Streptomycin.

Patients and transplant procedures

Patients and donors provided informed written consent for research, and studies were approved by the MSKCC Institutional Review Board. Of 267 total adult patients receiving HCT at MSKCC between 2006 to 2017 as part of a larger study (25), 20 patients who received a CD34+ selected graft (CliniMACS, Miltenyi) were analyzed further and included here. Patients did not receive additional pharmacologic GVHD prophylaxis. All patients received acyclovir prophylaxis starting on admission for HCT and continued for at least 12 months, and recipients who were CMV+ or CMV- with a CMV+ donor were routinely monitored at least weekly starting on D14 post-HCT. CMV infection/reactivation was determined by pp65 antigenemia assays prior to 2010 and by CMV qPCR (Roche Diagnostics) from 2010 onward.

Functional assays

Degranulation of NK cells was assessed by labeling with CD107a antibody in culture. IFNγ production was measured by blocking Golgi transport with brefeldin A (MP Biomedicals) and GolgiStop (BD) 1 hour after stimulation, followed by intracellular staining four hours later unless otherwise indicated. Replicates with fewer than 100 cells in the selected populations were excluded.

Co-culture with tumor cell targets was performed at a ratio of 1:1 PBMCs to Target cells in 100 µL. ADCC assays were performed with BE(2)n cells labeled with 1 µg/mL of the anti-GD2 clone 3F8 (provided by Dr. Nai-Kong Cheung). IFNγ production was also assessed following stimulation with 50 ng/mL PMA (Sigma) and 1 µg/mL ionomycin (MP Biomedicals). PBMCs were pre-treated with 200 U/mL of IL-2 (Peprotech) overnight as indicated.

For proliferation assays, PBMC were labeled with (1.66 µM) CTV and plated 250,000 per well and rested overnight, before stimulation with 0.625 ng/mL PMA and 0.5 µg/mL ionomycin.

Single-cell RNA sequencing

PBMCs from two CMV+ donors with two intact alleles of *KLRC2* were thawed and sorted as shown in Supplementary Figure S2A; Donor 1 is female, and Donor 2 is male. Sorted populations were labeled with TotalSeq-B Anti-Human Hashtag antibodies (Biolegend), and 3,000 cells from each of the seven sorted populations were combined for each donor and submitted to MSKCC's Integrated Genomic Operation core facility for 10x Genomics library prep and 3' Gene Expression and 5' Feature Barcode sequencing. The software Cell Ranger (version 5.0.1; 10x Genomics) was used for demultiplexing and alignment using default parameters. Velocyto (version 0.17.17) performed counting of spliced and un-spliced RNA molecules. Pre-processing and quality control of the data were carried out using the Python software package SCANPY (version 1.8.1). Cells that expressed low gene numbers, reading depth (counts) or high mitochondrial or ribosomal gene percentage were removed, the borders for these parameters were adapted according to the experiment. Cell cycle and mitochondrial genes were regressed out. SCANPY was also used to perform dimensionality reduction and clustering. The neighborhood graphs were based on 40 principal components and 80 neighbors. Clustering was performed using the Leiden algorithm with resolution r = 1.1. UMAP dimensionality reduction was computed using SCANPY's default parameters. The software tool scvelo (version 0.2.2) was used to compute RNA velocities within a deterministic model.

Statistical analysis

Statistical analyses were performed in GraphPad Prism 7.00 as described in the legends. Bars represent mean and SD; * $p < 0.05$, ** $p < 0.01$, *** $p < 0.001$, **** $p < 0.0001$.

Data availability statement

The datasets presented in this study can be found in online repositories. The names of the repository/repositories and accession number(s) can be found below: https://www.ncbi.nlm.nih.gov/geo/, GSE243030.

Ethics statement

The requirement of ethical approval was waived by Memorial Sloan Kettering Cancer Center IRB for the studies on humans because PBMCs were obtained from anonymized donors from the New York Blood Center. The studies were conducted in accordance with the local legislation and institutional requirements. Written informed consent for participation was not required from the participants or the participants' legal guardians/next of kin in accordance with the national legislation and institutional requirements. The human samples used in this study were acquired from a by- product of routine care or industry.

Author contributions

MKP: Conceptualization, Formal analysis, Investigation, Methodology, Writing – original draft, Writing – review & editing. SG: Formal analysis, Methodology, Writing – review & editing. RS: Investigation, Writing – review & editing. J-BLL: Investigation, Writing – review & editing. TK: Investigation, Writing – review & editing. KvdP: Investigation, Writing – review & editing. JCS: Supervision, Writing – review & editing. KCH: Conceptualization, Funding acquisition, Supervision, Writing – review & editing.

Funding

The author(s) declare financial support was received for the research, authorship, and/or publication of this article. These studies were funded by NIH R01 AI150999 and U01 AI069197, and the MSKCC Human Oncology and Pathogenesis Program. SG is the recipient of a CRI/Donald J. Gogel Fellowship (CRI #3934).

Acknowledgments

The authors would like to thank Drs. Lewis L. Lanier, Kyle B. Lupo, Gianluca Scarno, and Sanam Shahid for thoughtful feedback on the manuscript.

Conflict of interest

MKP and KCH are inventors on a patent application for the design and use of HLA-E:peptide chimeric molecules. KCH is a scientific advisory board member for Wugen, Inc., and a consultant for Exelixis.

The remaining authors declare that the research was conducted in the absence of any commercial or financial relationships that could be construed as a potential conflict of interest.

Publisher's note

Supplementary material

The Supplementary Material for this article can be found online at: https://www.frontiersin.org/articles/10.3389/fimmu.2024.1499492/full#supplementary-material

SUPPLEMENTARY FIGURE 1
Genetic and functional characteristics of the immature NKG2C+ precursor for adaptive NK cells. **(A)** Top, frequency of A+C+ among indicated populations according to *KLRC2* copy number; Mann-Whitney test performed. **(B)** MFI of NKGC in indicated NK cell populations among CMV- (left) and CMV+ (right) healthy individuals; Dunn's multiple comparison test performed, comparing groups below tick marks to group below capped end. **(C)** MFI of CD94 in indicated NK cell populations; Dunn's multiple comparison test performed, comparing groups below tick marks to group below capped end. **(D)** Degranulation and IFNγ production of NK cell populations after 5-hour co-culture with the indicated tumor cell lines. Dunn's multiple comparison test performed, comparing groups below tick marks to group below capped end. **(E)** Percentage change in degranulation and IFNγ production of NK cell populations in co-culture with K562 cells expressing HLA-E:peptide complexes relative to non-transduced K562 cells. Wilcoxon test performed on indicated pairs.

SUPPLEMENTARY FIGURE 2
Single-cell transcriptional profiling of phenotypically distinct NK cell populations. **(A)** Left, schematic of single-cell RNA sequencing experimental design. Right, sorting strategy for NK cell populations as represented on one of the two healthy donors. **(B)** Left, UMAP representation of peripheral blood NK cells from second donor, color-coded according to phenotypic population hashtag. Right, individual phenotypic populations superimposed on total NK. **(C)** Left, UMAP representation of peripheral blood NK cells from second donor, color-coded according to transcriptional cluster. **(D)** Phenotypic composition of transcriptional clusters from Donor 1. **(E)** RNA velocity analysis of Donor 1, color-coded according to transcriptional cluster.

SUPPLEMENTARY FIGURE 3
Transcriptomic profile shared by NKG2C+ CD56^{bright} and Adaptive NK cells. **(A)** UMAP of representative donor after removal of phenotypic CD56^{bright} cells (left) or A-C+ cells (right), color-coded according to phenotype (left) or transcriptional cluster (right). **(B)** Dot plot of selected DEGs in the indicated phenotypic populations in Donor 2. **(C)** Violin plots of selected gene expression in the indicated phenotypic populations in Donor 2; 25-75% IQR and median indicated by box and white dot, respectively. **(D)** Number of genes for ribosomal proteins upregulated or downregulated in the populations of individual donors.

SUPPLEMENTARY FIGURE 4
Adaptive Phenotype Present in NKG2C- NK Cell Populations of CMV-Seropositive Individuals. **(A)** Frequency of FcRγ- NK cells among different CD56^{dim} population (left), and MFI of FcRγ expression among FcRγ+ cells among NK cell populations (right); t-tests comparing CMV- and CMV+ individuals per population performed using Holm-Sidak method without assuming identical SD; N = 30 CMV- and 112 CMV+ *KLRC2*+ healthy donors. **(B)** Expression of surface markers in FcRγ+ and FcRγ- NK cells from CD56^{dim} NK populations; Sidak's multiple comparison test performed following 2-way paired ANOVA between FcRγ+ and FcRγ- cells within each population; N = 10 CMV+ *KLRC2*+ healthy donors.

SUPPLEMENTARY TABLE 1
DEGs by transcriptional cluster and by comparison.

References

1. Burnet SFM. *The clonal selection theory of acquired immunity* Vol. 3. Nashville, TN, USA: Vanderbilt University Press Nashville (1959).

2. Sun JC, Beilke JN, Lanier LL. Adaptive immune features of natural killer cells. *Nature*. (2009) 457(7229):557–61. doi: 10.1038/nature07665

3. Gumá M, Angulo A, Vilches C, Gómez-Lozano N, Malats N, López-Botet M. Imprint of human cytomegalovirus infection on the NK cell receptor repertoire. *Blood*. (2004) 104(12):3664–71. doi: 10.1182/blood-2004-05-2058

4. Gumá M, Budt M, Sáez A, Brckalo T, Hengel H, Angulo A, et al. Expansion of CD94/NKG2C+ NK cells in response to human cytomegalovirus-infected fibroblasts. *Blood*. (2006) 107(9):3624–31. doi: 10.1182/blood-2005-09-3682

5. Béziat V, Liu LL, Malmberg JA, Ivarsson MA, Sohlberg E, Björklund AT, et al. NK cell responses to cytomegalovirus infection lead to stable imprints in the human KIR repertoire and involve activating KIRs. *Blood*. (2013) 121(14):2678–88. doi: 10.1182/blood-2012-10-459545

6. Arase H, Mocarski ES, Campbell AE, Hill AB, Lanier LL. Direct recognition of cytomegalovirus by activating and inhibitory NK cell receptors. *Science*. (2002) 296 (5571):1323–6. doi: 10.1126/science.1070884

7. Smith HRC, Heusel JW, Mehta IK, Kim S, Dorner BG, Naidenko OV, et al. Recognition of a virus-encoded ligand by a natural killer cell activation receptor. *Proc Natl Acad Sci*. (2002) 99(13):8826–31. doi: 10.1073/pnas.092258599

8. Prod'homme V, Tomasec P, Cunningham C, Lemberg MK, Stanton RJ, McSharry BP, et al. Human cytomegalovirus UL40 signal peptide regulates cell surface expression of the NK cell ligands HLA-E and gpUL18. *J Immunol*. (2012) 188:2794–804. doi: 10.4049/jimmunol.1102068

9. Hammer Q, Rückert T, Borst EM, Dunst J, Haubner A, Durek P, et al. Peptide-specific recognition of human cytomegalovirus strains controls adaptive natural killer cells. *Nat Immunol*. (2018) 19:453–63. doi: 10.1038/s41590-018-0082-6

10. Rückert T, Lareau CA, Mashreghi M-F, Ludwig LS, Romagnani C. Clonal expansion and epigenetic inheritance of long-lasting NK cell memory. *Nat Immunol*. (2022) 23:1551–63. doi: 10.1038/s41590-022-01327-7

11. Lopez-Vergès S, Milush JM, Schwartz BS, Pando MJ, Jarjoura J, York VA, et al. Expansion of a unique $CD57^{+}NKG2C^{hi}$ natural killer cell subset during acute human cytomegalovirus infection. *Proc Natl Acad Sci*. (2011) 108:14725–32. doi: 10.1073/pnas.1110900108

12. Liu LL, Landskron J, Ask EH, Enqvist M, Sohlberg E, Traherne JA, et al. Critical role of CD2 co-stimulation in adaptive natural killer cell responses revealed in NKG2C-deficient humans. *Cell Rep*. (2016) 15:1088–99. doi: 10.1016/j.celrep.2016.04.005

13. Schlums H, Cichocki F, Tesi B, Theorell J, Beziat V, Holmes TD, et al. Cytomegalovirus infection drives adaptive epigenetic diversification of NK cells with altered signaling and effector function. *Immunity*. (2015) 42:443–56. doi: 10.1016/j.immuni.2015.02.008

14. Lee J, Zhang T, Hwang I, Kim A, Nitschke L, Kim M, et al. Epigenetic modification and antibody-dependent expansion of memory-like NK cells in human cytomegalovirus-infected individuals. *Immunity*. (2015) 42:431–42. doi: 10.1016/j.immuni.2015.02.013

15. Horowitz A, Strauss-Albee DM, Leipold M, Kubo J, Nemat-Gorgani N, Dogan OC, et al. Genetic and environmental determinants of human NK cell diversity revealed by mass cytometry. *Sci Trans Med*. (2013) 5:208ra145. doi: 10.1126/scitranslmed.3006702

16. Rebuffet L, Melsen JE, Escalière B, Basurto-Lozada D, Bhandoola A, Björkström NK, et al. High-dimensional single-cell analysis of human natural killer cell heterogeneity. *Nat Immunol*. (2024) 25:1474–88. doi: 10.1038/s41590-024-01883-0

17. Netskar H, Pfefferle A, Goodridge JP, Sohlberg E, Dufva O, Teichmann SA, et al. Pan-cancer profiling of tumor-infiltrating natural killer cells through transcriptional reference mapping. *Nat Immunol*. (2024) 25:1445–59. doi: 10.1101/2023.10.26.564050

18. Jaeger N, Antonova AU, Kreisel D, Roan F, Lantelme E, Ziegler SF, et al. Diversity of group 1 innate lymphoid cells in human tissues. *Nat Immunol*. (2024) 25:2460–1473. doi: 10.1038/s41590-024-01885-y

19. Brenchley JM, Karandikar NJ, Betts MR, Ambrozak DR, Hill BJ, Crotty LE, et al. Expression of CD57 defines replicative senescence and antigen-induced apoptotic death of CD8+ T cells. *Blood*. (2003) 101:2711–20. doi: 10.1182/blood-2002-07-2103

20. Tarazona R, DelaRosa O, Alonso C, Ostos B, Espejo J, Peña J, et al. Increased expression of NK cell markers on T lymphocytes in aging and chronic activation of the immune system reflects the accumulation of effector/senescent T cells. *Mech Ageing Dev*. (2000) 121:77–88. doi: 10.1016/S0047-6374(00)00199-8

21. Lopez-Vergès S, Milush JM, Pandey S, York VA, Arakawa-Hoyt J, Pircher H, et al. CD57 defines a functionally distinct population of mature NK cells in the human CD56dimCD16+ NK-cell subset. *Blood*. (2010) 116:3865–74. doi: 10.1182/blood-2010-04-282301

22. Sallusto F, Lenig D, Förster R, Lipp M, Lanzavecchia A. Two subsets of memory T lymphocytes with distinct homing potentials and effector functions. *Nature*. (1999) 402:34–8. doi: 10.1038/35005534

23. Juelke K, Killig M, Luetke-Eversloh M, Parente E, Gruen J, Morandi B, et al. CD62L expression identifies a unique subset of polyfunctional CD56dim NK cells. *Blood*. (2010) 116:1299–307. doi: 10.1182/blood-2009-11-253286

24. Frey M, Packianathan NB, Fehniger TA, Ross ME, Wang WC, Stewart CC, et al. Differential expression and function of L-selectin on CD56bright and CD56dim natural killer cell subsets. *J Immunol*. (1998) 161:400–8. doi: 10.4049/jimmunol.161.1.400

25. Van Der Ploeg K, Sottile R, Kontopoulos T, Shaffer BC, Papanicolaou GA, Maloy MA, et al. Emergence of Human CMV-induced NKG2C+ NK cells is Associated with CD8+ T cell Recovery following Allogeneic HCT. *Blood Adv*. (2023) 7(19):5784–98. doi: 10.1182/bloodadvances.2022008952

26. Sáez-Borderías A, Romo N, Gumá Mn Magri G, Angulo A, López-Botet M. IL-12-dependent inducible expression of the CD94/NKG2A inhibitory receptor regulates CD94/NKG2C+ NK cell function1. *J Immunol*. (2009) 182:829–36. doi: 10.4049/jimmunol.182.2.829

27. Björkström NK, Riese P, Heuts F, Andersson S, Fauriat C, Ivarsson MA, et al. Expression patterns of NKG2A, KIR, and CD57 define a process of CD56dim NK-cell differentiation uncoupled from NK-cell education. *Blood*. (2010) 116:3853–64. doi: 10.1182/blood-2010-04-281675

28. Béziat V, Descours B, Parizot C, Debré P, Vieillard V. NK cell terminal differentiation: correlated stepwise decrease of NKG2A and acquisition of KIRs. *PloS One*. (2010) 5:e11966. doi: 10.1371/journal.pone.0011966

29. Braud VM, Allan DSJ, CA, Söderström K, O'Callaghan A, Ogg GS, et al. HLA-E binds to natural killer cell receptors CD94/NKG2A, B and C. *Nature*. (1998) 391:795–9. doi: 10.1038/35869

30. Shemesh A, Su Y, Calabrese DR, Chen D, Arakawa-Hoyt J, Roybal KT, et al. Diminished cell proliferation promotes natural killer cell adaptive-like phenotype by limiting FcεRIγ expression. *J Exp Med*. (2022) 219. doi: 10.1084/jem.20220551

31. Ishiyama K, Arakawa-Hoyt J, Aguilar OA, Damm I, Towfighi P, Sigdel T, et al. Mass cytometry reveals single-cell kinetics of cytotoxic lymphocyte evolution in CMV-infected renal transplant patients. *Proc Natl Acad Sci*. (2022) 119:e2116588119. doi: 10.1073/pnas.2116588119

32. Wu Z, Lau CM, Sottile R, Luduec Le JB, Panjwani MK, Conaty PM, et al. Human cytomegalovirus infection promotes expansion of a functionally superior cytoplasmic CD3(+) NK cell subset with a bcl11b-regulated T cell signature. *J Immunol*. (2021) 207(10):2534–44. doi: 10.4049/jimmunol.2001319

33. Gutierrez-Arcelus M, Teslovich N, Mola AR, Polidoro RB, Nathan A, Kim H, et al. Lymphocyte innateness defined by transcriptional states reflects a balance between proliferation and effector functions. *Nat Commun*. (2019) 10:687. doi: 10.1038/s41467-019-08604-4

34. Carty SA, Gohil M, Banks LB, Cotton RM, Johnson ME, Stelekati E, et al. The loss of TET2 promotes CD8+ T cell memory differentiation. *J Immunol*. (2018) 200:82–91. doi: 10.4049/jimmunol.1700559

35. Ma S, Wan X, Deng Z, Shi L, Hao C, Zhou Z, et al. Epigenetic regulator CXXC5 recruits DNA demethylase Tet2 to regulate TLR7/9-elicited IFN response in pDCs. *J Exp Med*. (2017) 214:1471–91. doi: 10.1084/jem.20161149

36. Ko M, An J, Bandukwala HS, Chavez L, Äijö T, Pastor WA, et al. Modulation of TET2 expression and 5-methylcytosine oxidation by the CXXC domain protein IDAX. *Nature*. (2013) 497:122–6. doi: 10.1038/nature12052

37. Tsuchiya Y, Naito T, Tenno M, Maruyama M, Koseki H, Taniuchi I, et al. ThPOK represses CXXC5, which induces methylation of histone H3 lysine 9 in Cd40lg promoter by association with SUV39H1: implications in repression of CD40L expression in CD8+ cytotoxic T cells. *J Leukocyte Biol*. (2016) 100:327–38. doi: 10.1189/jlb.1A0915-396RR

38. Fraietta JA, Nobles CL, Sammons MA, Lundh S, Carty SA, Reich TJ, et al. Disruption of TET2 promotes the therapeutic efficacy of CD19-targeted T cells. *Nature*. (2018) 558:307–12. doi: 10.1038/s41586-018-0178-z

39. Pace L, Goudot C, Zueva E, Gueguen P, Burgdorf N, Waterfall JJ, et al. The epigenetic control of stemness in CD8(+) T cell fate commitment. *Science*. (2018) 359:177–86. doi: 10.1126/science.aah6499

40. Cooper MA, Fehniger TA, Turner SC, Chen KS, Ghaheri BA, Ghayur T, et al. Human natural killer cells: a unique innate immunoregulatory role for the CD56 (bright) subset. *Blood*. (2001) 97:3146–51. doi: 10.1182/blood.V97.10.3146

41. Elpek KG, Rubinstein MP, Bellemare-Pelletier A, Goldrath AW, Turley SJ. Mature natural killer cells with phenotypic and functional alterations accumulate upon sustained stimulation with IL-15/IL-15Ralpha complexes. *Proc Natl Acad Sci U.S.A*. (2010) 107:21647–52. doi: 10.1073/pnas.1012128107

42. Kritikou JS, Oliveira MM, Record J, Saeed MB, Nigam SM, He M, et al. Constitutive activation of WASp leads to abnormal cytotoxic cells with increased granzyme B and degranulation response to target cells. *JCI Insight*. (2021) 6. doi: 10.1172/jci.insight.140273

43. Goodridge JP, Jacobs B, Saetersmoen ML, Clement D, Hammer Q, Clancy T, et al. Remodeling of secretory lysosomes during education tunes functional potential in NK cells. *Nat Commun*. (2019) 10:514. doi: 10.1038/s41467-019-08384-x

44. Wu Z, Park S, Lau CM, Zhong Y, Sheppard S, Sun JC, et al. Dynamic variability in SHP-1 abundance determines natural killer cell responsiveness. *Sci Signaling*. (2021) 14:eabe5380. doi: 10.1126/scisignal.abe5380

45. Harding FA, McArthur JG, Gross JA, Raulet DH, Allison JP. CD28-mediated signalling co-stimulates murine T cells and prevents induction of anergy in T-cell clones. *Nature*. (1992) 356:607–9. doi: 10.1038/356607a0

46. Kedl RM, Mescher MF. Qualitative differences between naive and memory T cells make a major contribution to the more rapid and efficient memory CD8+ T cell response. *J Immunol*. (1998) 161:674–83. doi: 10.4049/jimmunol.161.2.674

47. Cooper MA, Elliott JM, Keyel PA, Yang L, Carrero JA, Yokoyama WM. Cytokine-induced memory-like natural killer cells. *Proc Natl Acad Sci U.S.A*. (2009) 106:1915–9. doi: 10.1073/pnas.0813192106

48. Romee R, Schneider SE, Leong JW, Chase JM, Keppel CR, Sullivan RP, et al. Cytokine activation induces human memory-like NK cells. *Blood*. (2012) 120:4751. doi: 10.1182/blood-2012-04-419283

49. Berrien-Elliott MM, Foltz JA, Russler-Germain DA, Neal CC, Tran J, Gang M, et al. Hematopoietic cell transplantation donor-derived memory-like NK cells functionally persist after transfer into patients with leukemia. *Sci Trans Med*. (2022) 14:eabm1375. doi: 10.1126/scitranslmed.abm1375

50. Foltz JA, Tran J, Wong P, Fan C, Schmidt E, Fisk B, et al. Cytokines drive the formation of memory-like NK cell subsets via epigenetic rewiring and transcriptional regulation. *Sci Immunol*. (2024) 9:eadk4893. doi: 10.1126/sciimmunol.adk4893

51. Sottile R, Panjwani MK, Lau CM, Daniyan AF, Tanaka K, Barker JN, et al. Human cytomegalovirus expands a $CD8^{+}$ T cell population with loss of BCL11B expression and gain of NK cell identity. *Sci Immunol*. (2021) 6:eabe6968. doi: 10.1126/sciimmunol.abe6968

52. Ding Y, Lavaert M, Grassmann S, Band VI, Chi L, Das A, et al. Distinct developmental pathways generate functionally distinct populations of natural killer cells. *Nat Immunol*. (2024) 25:1183–92. doi: 10.1038/s41590-024-01865-2

53. Opferman JT, Ober BT, Ashton-Rickardt PG. Linear differentiation of cytotoxic effectors into memory T lymphocytes. *Science*. (1999) 283:1745–8. doi: 10.1126/science.283.5408.1745

54. Kaech SM, Hemby S, Kersh E, Ahmed R. Molecular and functional profiling of memory CD8 T cell differentiation. *Cell*. (2002) 111:837–51. doi: 10.1016/S0092-8674(02)01139-X

55. Wherry EJ, Teichgräber V, Becker TC, Masopust D, Kaech SM, Antia R, et al. Lineage relationship and protective immunity of memory CD8 T cell subsets. *Nat Immunol*. (2003) 4:225–34. doi: 10.1038/ni889

56. Manjunath N, Shankar P, Wan J, Weninger W, Crowley MA, Hieshima K, et al. Effector differentiation is not prerequisite for generation of memory cytotoxic T lymphocytes. *J Clin Invest*. (2001) 108:871–8. doi: 10.1172/JCI13296

57. Grassmann S, Mihatsch L, Mir J, Kazeroonian A, Rahimi R, Flommersfeld S, et al. Early emergence of T central memory precursors programs clonal dominance during chronic viral infection. *Nat Immunol*. (2020) 21:1563–73. doi: 10.1038/s41590-020-00807-y

58. Kaech SM, Cui W. Transcriptional control of effector and memory CD8+ T cell differentiation. *Nat Rev Immunol*. (2012) 12:749–61. doi: 10.1038/nri3307

59. Lanzavecchia A, Sallusto F. Progressive differentiation and selection of the fittest in the immune response. *Nat Rev Immunol*. (2002) 2:982–7. doi: 10.1038/nri959

60. Chang JT, Palanivel VR, Kinjyo I, Schambach F, Intlekofer AM, Banerjee A, et al. Asymmetric T lymphocyte division in the initiation of adaptive immune responses. *Science*. (2007) 315:1687–91. doi: 10.1126/science.1139393

61. Ciocca ML, Barnett BE, Burkhardt JK, Chang JT, Reiner SL. Cutting edge: asymmetric memory T cell division in response to rechallenge. *J Immunol*. (2012) 188:4145–8. doi: 10.4049/jimmunol.1200176

62. Netea MG, Domínguez-Andrés J, Barreiro LB, Chavakis T, Divangahi M, Fuchs E, et al. Defining trained immunity and its role in health and disease. *Nat Rev Immunol*. (2020) 20:375–88. doi: 10.1038/s41577-020-0285-6

63. Miyashita R, Tsuchiya N, Hikami K, Kuroki K, Fukazawa T, Bijl M, et al. Molecular genetic analyses of human NKG2C (KLRC2) gene deletion. *Int Immunol*. (2004) 16:163–8. doi: 10.1093/intimm/dxh013